■  6329

# Study on Control Strategies for the Multilevel Cascaded Converters

**Lin Xu*[1], Yang Han[2]**

[1]Sichuan Electric Power Research Institute, No.24, Qinghua Road, Qingyang District, 610072 Chengdu, China
[2]University of Electronic Science and Technology of China, No.2006, Xiyuan Road, West High-Tech Zone, Chengdu, 611731, Chengdu, China
*Corresponding author, e-mail: xulin198431@hotmail.com

*Abstract*

*The multilevel cascaded converters are extensively applied for high-voltage and high-power applications, which are considered as the most favorable topologies for the high power ac-drives and the high-voltage DC transmission (HVDC) systems using the voltage source converters (VSCs). This paper presents the dc capacitor balancing and effective current regulation methodologies for the multilevel cascaded converters. The dc-link voltage balancing and capacitor energy evolving mechanism of the MMCC is analyzed, and an effective control scheme is devised by utilizing two dc capacitor voltage control loops, including the total capacitor voltage controller (TCVC), the capacitor voltage balancing controller (CVBC). The predictive current controller is proposed to enhance the tracking accuracy of current control loop. The proportional-resonant controller (PRC) is used as circulating current damping controller of the modular multilevel converter, which is found to be highly effective to minimize the circulating current. The Electromagnetic Transient Program (EMTP) is utilized for digital simulation of the single-phase five-level modular multilevel converter. The effectiveness of the control scheme is validated by the simulation results.*

*Keywords: multilevel converter, predictive current control, Dc-link control, EMTP*

## 1. Introduction

Multilevel voltage-source converters (VSCs) allow a significant reduction of the harmonic content of the output voltage as compared to the traditional two-level VSCs [1]. Among various multilevel topologies [2], the fairly recently proposed modular multilevel cascade converter (MMCC) [3] has many attractive properties. As the name suggests, the topology is modular and easily scalable in terms of voltage levels. It consists of N identical series-connected sub-modules per arm, which brings flexibility to the circuit design, and results in low-voltage steps [4, 5].

In high-voltage applications, N may be as high as several hundred, which is ideal choice for high-voltage high-power applications, such as high-voltage dc transmission (HVDC), high-power motor drives, and electric railway supplies [5-8]. The grid-connected MMCC may act as a rectifier, an inverter, an inductor, and a capacitor, depending on the phase difference between the supply voltage and current. This implies that the MMCC is required to achieve rigid and stable voltage control of all the floating dc capacitors under all operating conditions.

This paper presents the dc-link capacitor balancing and effective current regulation methodologies for the MMCC. The organization of this paper is as follows. Section 2 presents the system description of the MMCC system, including the modeling and analysis of the MMCC. Section 3 presents the control strategies of the MMCC, including the sum capacitor voltage controller (SCVC), the difference capacitor voltage controller (DCVC), the predictive current loop controller (PCC) and the circulating current damping controller (CCDC). Section 4 presents the simulation results. And section 5 concludes this paper.

## 2. Mathematical Modeling for Modular Multilevel Converter

Figure 1 shows the circuit diagram of the single-phase modular multilevel cascaded converter (MMCC). To derive the mathematical model of the MMC converter, let us consider a generic converter with N sub-modules per arm, each arm is controlled with the modulation index $m(t)$, where $m(t)=0$ means that all sub-modules in the arm are by-passed, and $m(t)=1$ denotes all the sub-modules in the arm are inserted. The ideal capacitance of the arm is denoted as:

$$C_{u,d} = C_{dc} / N \tag{1}$$



Figure 1. Circuit Diagram of the Single-phase MMCC Topology

Where $C_{u,d}$ denotes the capacitance of each chopper cell. Therefore, the following equations hold for the upper and lower leg currents:

$$\frac{d\sum u_{dc,u}(t)}{dt} = \frac{m_u(t)i_u(t)}{C_u} \tag{2}$$

$$\frac{d\sum u_{dc,d}(t)}{dt} = \frac{m_d(t)i_d(t)}{C_d} \tag{3}$$

Where $m_u(t)$ and $m_d(t)$, $u_{dc,u}(t)$ and $u_{dc,d}(t)$, $i_u(t)$ and $i_d(t)$ denote the modulation index, the capacitor voltages and currents of the upper and lower arm, respectively.

Referring to Figure 1, when only the single-phase leg is considered, the relations among $i_u$, $i_d$ and the circulating current $i_{z0}$ can be derived as:

$$i_{z0} = \frac{i_u + i_d}{2}, \quad i_u = \frac{i_L}{2} + i_{z0}, \quad i_d = -\frac{i_L}{2} + i_{z0} \tag{4}$$

Hence, the load current is represented as:

$$i_L = i_u - i_d \tag{5}$$

From Figure 1, according to the Kirchhoff's Voltage Law (KVL):

$$\frac{V_d}{2} - R_e i_u - L_e \frac{di_u}{dt} - m_u \sum u_{dc,u} = u_v \tag{6}$$

$$-\frac{V_d}{2} + R_e i_d + L_e \frac{di_d}{dt} + m_d \sum u_{dc,d} = u_v \tag{7}$$

Where $u_v$ denotes the voltage at the center of the converter leg, and $R_e$ and $L_e$ denote the effective series resistance and buffer inductance for each arm.
From Equation (6) and Equation (7), we get:

$$u_{z0} = R_e i_{z0} + L_e \frac{di_{z0}}{dt} = \frac{V_d}{2} - \frac{m_u \sum u_{dc,u} + m_d \sum u_{dc,d}}{2} \tag{8}$$

$$u_v = \frac{m_u \sum u_{dc,u} - m_d \sum u_{dc,d}}{2} - \frac{R_e}{2} i_L - \frac{L_e}{2} \frac{di_L}{dt} \tag{9}$$

Where $u_{z0}$ denotes the voltage drop across the $R_e$ and $L_e$ due to the circulating current $i_{z0}$. From Equation (8) and Equation (9), we get:

$$\frac{d[\sum u_{dc,u}(t) + \sum u_{dc,d}(t)]}{dt} = \frac{N}{C_{dc}}(m_u i_u + m_d i_d) \tag{10}$$

$$\frac{d[\sum u_{dc,u}(t) - \sum u_{dc,d}(t)]}{dt} = \frac{N}{C_{dc}}(m_u i_u - m_d i_d) \tag{11}$$

The modulation index $m_u$ and $m_d$ can be denoted as:

$$m_u = \frac{1}{2} - \frac{u_v + u_{z0}}{V_d}, m_d = \frac{1}{2} + \frac{u_v - u_{z0}}{V_d} \tag{12}$$

Let:

$$\sum u_{dc,u}(t) + \sum u_{dc,d}(t) = \sum u_{dc}(t) \tag{13}$$

$$\sum u_{dc,u}(t) - \sum u_{dc,d}(t) = \Delta u_{dc}(t) \tag{14}$$

Substituting Equation (12)-(14) into Equation (9)-(10), we get:

$$\frac{d \sum u_{dc}(t)}{dt} = \frac{N}{C_{dc}} [-\frac{u_v i_L}{V_d} + (1 - \frac{2u_{z0}}{V_d}) i_{z0}] \tag{15}$$

$$\frac{d \Delta u_{dc}(t)}{dt} = \frac{N}{C_{dc}} [(\frac{1}{2} - \frac{u_{z0}}{V_d}) i_L - \frac{2u_v i_{z0}}{V_d}] \tag{16}$$

From Equation (8), we get:

$$L_e \frac{di_{z0}}{dt} = \frac{V_d}{2} - \frac{m_u \sum u_{dc,u} + m_d \sum u_{dc,d}}{2} - R_e i_{z0} \tag{17}$$

The second term can be denoted as:

$$\frac{1}{2}(m_u \sum u_{dc,u} + m_d \sum u_{dc,d}) = (\frac{1}{4} - \frac{u_{z0}}{2V_d}) \sum u_{dc}(t) - \frac{u_v}{V_d} \Delta u_{dc}(t) \tag{18}$$

Hence, Equation (17) can be rewritten as:

$$\frac{di_{z0}}{dt} = \frac{V_d}{2L_e} - (\frac{1}{4L_e} - \frac{u_{z0}}{2V_d L_e}) \sum u_{dc}(t) - \frac{u_v}{V_d L_e} \Delta u_{dc}(t) - \frac{R_e}{L_e} i_{z0} \tag{19}$$

Notably, the MMCC system dynamics can be described by Equation (15)-(19), and the theoretical steady state point can be derived. However, since the coefficients in these differential equations are time-varying, the analytical solution would not be directly obtained. Whereas, the approximated steady state solution of $i_{z0}$ can be derived from Equation (19) by assuming the $u_{z0}$ is small compared with $V_d$, thus we get:

$$i_{z0} = \frac{u_v i_L}{V_d} \tag{20}$$

Substituting Equation (20) to Equation (16), the $u_{z0}$ is derived as:

$$u_{z0} = \frac{V_d}{2} - \frac{2u_v^2}{V_d} \tag{21}$$

The output voltage $u_v$ can be approximated as:

$$u_v = V_m \sin(\omega t) \tag{22}$$

In case of active rectifier mode, $i_L$ can be approximated as:

$$i_L = I_m \sin(\omega t) \tag{23}$$

Hence, $i_{z0}$ can be derived as:

$$i_{z0} = \frac{V_m I_m}{2V_d}(1 - \cos(2\omega t)) \tag{24}$$

And $u_{z0}$ is rewritten as:

$$u_{z0} = \frac{V_d}{2} - \frac{V_m^2}{V_d}(1 - \cos(2\omega t)) \tag{25}$$

In case of reactive power generation mode, $i_L$ is denoted as:

$$i_L = I_m \sin(\omega t - 90°) \tag{26}$$

Hence, $i_{z0}$ can be derived as:

$$i_{z0} = \frac{V_m I_m}{2V_d}\sin(2\omega t) \tag{27}$$

It can be observed from Equation (24)-(27) that, in either active rectifier or reactive compensation mode, $i_{z0}$ contains a second order oscillation term, which causes unnecessary circulating currents and power loss across the converter arms. This effect can be minimized by using damping controller based on the circulating current damping controller (CCDC).


## 3. Control Strategies of the Modular Multilevel Converter

The control strategy implemented is a linear control which aims to operate MMC in the proximity of the linear region. Two different voltage control loops are implemented, namely, the total capacitor voltage controller (TCVC) and the capacitor voltage balancing controller (CVBC), the TCVC block is used to control the overall energy of the leg, and the CVBC block is used to control the balance between upper and lower arms of the MMCC phase-leg. Notably, due to the non-linear system equations, the interaction between the TCVC and CVBC loops may lead to instability. However, since total energy and energy balance interacts dynamically, the TCVC loop is tuned to be about ten percent of the CVBC loop to achieve the decoupled control.

### 3.1. Total Capacitor Voltage Controller

The total capacitor voltage controller (TCVC) is used to regulate the total energy stored in a MMC converter leg. Typically, in a steady state operation, the reference value is set to $2V_d$. It has been found that the proportional controller $k_{p,sum}$ is sufficient to regulate the sum capacitor voltage to its reference. By adding an integration term, the TCVC control is also effective, but the parameter selection is crucial to ensure global stability under a wide operation range. For the sake of simplicity, the proportional control is a good tradeoff between the accuracy and robustness.

### 3.2. Capacitor Voltage Balancing Controller

Referring to Equation (16), the term $i_L$ is not producing any average value since it is an AC component in steady state. The term also $-2i_{z0}u_v/V_d$ contributes only by an oscillating term, if $i_{z0}$ does not have any component with the same frequency as $u_v$. The only quantity that can be freely varied without causing deviations from $u_v$ reference is $i_{z0}$. Therefore, the only way to influence the energy balance between the two arms is to regulate the circulating current $i_{z0}$. A separate proportional controller $k_{p,diff}$ is utilized to regulate the difference capacitor voltage to its reference (zero).

### 3.3. Predictive Current Controller (PCC)

Current control of the MMCC can be made with high bandwidth, which is crucial for reduction of transient currents during faults, and reduction of current harmonics. Both the output current $i_L$ and circulating current $i_{z0}$ are available for feedback control. The differential equation across the grid impedance is described as:

$$\frac{di_L}{dt} = -\frac{r_L}{L} \cdot i_L + \frac{1}{L}[u_v - v_g] \tag{28}$$

Where $L$ and $r_L$ denotes the grid coupling inductance and its equivalent resistance. Let $v(t) = u_v(t) - v_g(t)$, the following equation can be derived:

$$i_L(t) = e^{-\frac{r_L}{L}(t-t_0)} \cdot i_L(t_0) + \int_{t_0}^{t} e^{-\frac{r_L}{L}(t-\tau)} \frac{1}{L} v(\tau)d\tau \tag{29}$$

Notably, the control loop of the MMCC belongs to the typical sample-data control system. Let $t_0 = kT_s$, $t = (k+1)T_s$, the discrete representation of Equation (29) is derived as:

$$i_L(k+1) = e^{-\frac{r_L}{L}T_s} \cdot i_L(k) + \frac{1}{L}\int_{kT_s}^{(k+1)T_s} e^{-\frac{r_L}{L}[(k+1)T_s-\tau]} \cdot v(\tau)d\tau \tag{30}$$

Since $r_L$ is very small, hence we get $e^{-\frac{r_L}{L}[(k+1)T_s-\tau]} \approx 1$, thus the following equation can be obtained:

$$i_L(k+1) = e^{-\frac{r_L}{L}T_s} \cdot i_L(k) + \frac{1}{L}\int_{kT_s}^{(k+1)T_s} [u_v(\tau) - v_g(\tau)]d\tau \tag{31}$$

In order to derive the predictive current control, the reference current for $i_L(t)$ at the $k$th sampling instant is represented as $i_{ref}(k) = i_L(k+2)$, thus the MMCC output voltage $u_v$ is derived as:

$$u_v(k) = -\frac{L_m}{T_s}[i_{ref}(k) - e^{-r_L T_s/L_m} \cdot i_L(k+1)] + \bar{v}_g(k+1) \tag{32}$$

From Equation (32), it can be deduced that, in order to calculate the MMCC output voltage $u_v(k)$, it is necessary to predict the values $i_L(k+1)$ and the average value of $v_g(k+1)$. By using the interpolation method, the relations among the consecutive three sampling points of grid voltages are derived as:

$$v_g(k+2) = 2v_g(k+1) - v_g(k) \tag{33}$$

Thus, the last term in Equation (32) is denoted as:

$$\overline{v}_g(k+1) = \frac{1}{2}[v_g(k+1) + v_g(k+2)] = \frac{5}{2}v_g(k) - \frac{3}{2}v_g(k-1) \tag{34}$$

In order to predict $i_L(k+1)$, the variable $L$ in Eq.(31) is replaced by its nominal value $L_m$, thus:

$$i_L(k+1) = e^{-\frac{r_L}{L_m}T_s} \cdot i_L(k) + \frac{T_s}{L_m} \cdot [u_v(k-1) - \overline{v}_g(k)] \tag{35}$$

Therefore, the block diagram of the predictive current control law is derived as shown in Figure 2.
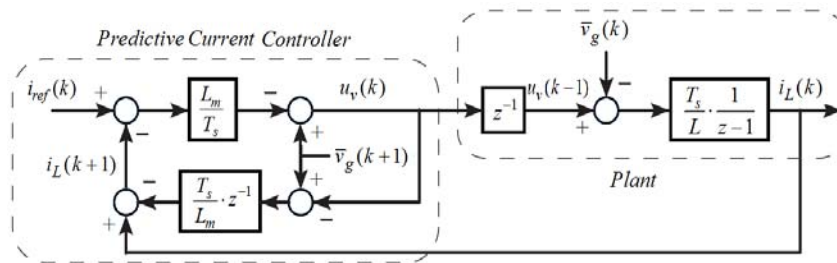


Figure 2. The Block Diagram of the Predictive Current Control Law

From the block diagram, the open-loop transfer function of the current controller $H(z)$ is obtained as:

$$H(z) = \frac{L_m}{L} \cdot \frac{1}{(z+1)(z-1)} \tag{36}$$

The closed-loop characteristic equation is $1+H(z)=0$, hence we get:

$$\frac{L_m + L(z^2 - 1)}{L(z^2 - 1)} = 0 \tag{37}$$

Therefore, the poles are represented as:

$$z = \pm\sqrt{(L - L_m)/L} \tag{38}$$

From Equation (38), it can be observed that, in case of $L=L_m$, we get $z^2=0$, indicating that the MMCC output current tracks the reference signal in two cycles.

### 3.4. Circulating Current Damping Controller (CCDC)

The proportional-integral regulator shows unsatisfactory performance for current tracking in case of alternating reference signal, which results in remarkable phase and amplitude tracking errors. The proportional resonant (PR) current controller, on the other hand, achieves excellent tracking performance for the alternating signal, which mimics the PI regulator implemented in the synchronous rotating reference frame (SRRF) with the following transfer function:

$$G_{PR}(s) = k_{p,z0} + \frac{k_{i,z0}}{s^2 + \omega_n^2} \qquad (39)$$

Where the parameters $k_{p,z0}$ and $k_{i,z0}$ are proportional and resonant gain, and $\omega_n$ denotes the angular frequency of the target alternating signal, which implies the second order harmonic in the present case. Thanks to the infinite open-loop gain introduced by the PR regulator, the zero steady-state tracking error is realized for the alternating signal at 100Hz.

## 4. Simulation Results and Discussions

To validate the effectiveness of the control strategies, the digital simulation of the single-phase five-level MMCC converter is carried out using the Electromagnetic Transient Program (EMTP-ATP). The system parameters are: the buffer inductance and resistance $L_e$=4.5mH, $R_e$=0.02Ohm, $V_d$=800V, the dc-link capacitor value $C_{dc}$=2.5mF, the grid inductance $L_s$=1.5mH, $V_{grid}$=220V (RMS), the capacitor reference dc-link voltage $V_{dc,ref}$=400V, the TCVC controller gain $k_{p,sum}$=12, the CVBC controller gain $k_{p,diff}$=1.2, the circulating current damping controller (CCDC) gain $k_{p,z0}$=1.5, $k_{i,z0}$=200.
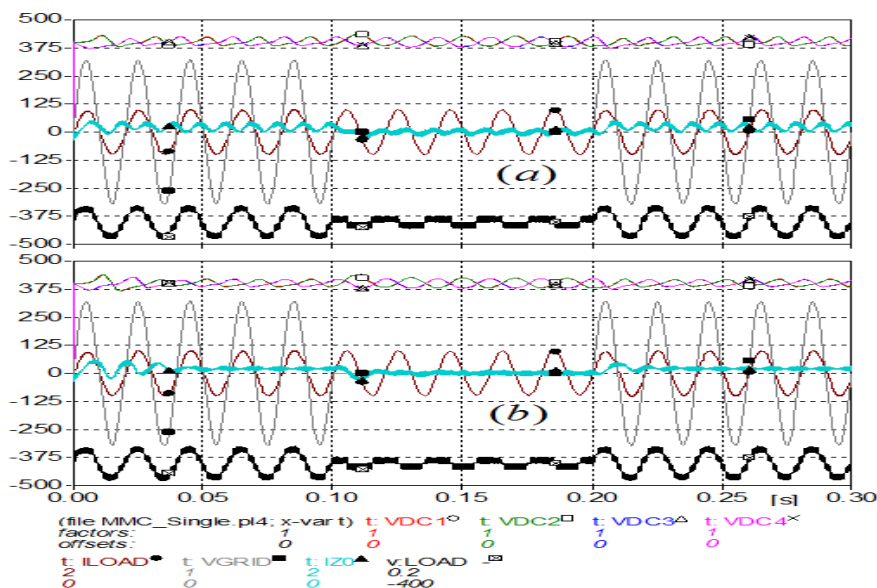


Figure 3. The Simulation Results of the MMCC under Active Rectifier Mode
(a) without and (b) with circulating current damping controller.

Figure 3 shows the simulation results of the MMCC under active rectifier mode. And the grid voltage undergoes outages during $t$=0.1s and $t$=0.2s. The dc-link capacitor voltages $u_{dc1} \sim u_{dc4}$, the load current $i_L$, the load voltage $v_{Load}$, the grid voltage $v_g$, and the circulating current $i_{z0}$ can be observed. In Figure 3, the peak active current reference $i_{L,ref}$=50A, it can be observed in Figure 3(a) that the dc-link capacitor voltages are stable both in steady state and transient process, and the circulating current $i_{z0}$ shows obvious second order oscillation with positive dc offset without the circulating current controller. However, when the circulating current controller is activated, the second order component is eliminated, as shown in Figure 3(b).

## 5. Conclusion

The dc capacitor balancing and effective current regulation methodologies for the modular multilevel cascaded converter (MMCC) are proposed in this paper. Based on the capacitor energy evolving mechanism, an effective capacitor control scheme is devised, which

includes the total capacitor voltage controller (TCVC) and capacitor voltage balancing controller (CVBC). To enhance the tracking accuracy of current control loop, the predictive current controller (PCC) is presented. To minimize the circulating current of the MMCC, an effective circulating current damping controller (CCDC) is proposed using proportional-resonant controller. The simulation results under active rectifier mode are presented for verification, which shows perfect capacitor voltage balancing control and precise current tracking.

**References**
[1]  M Hagiwara, H Akagi. Control and experiment of pulse-width modulated modular multilevel converters. *IEEE Trans. Power Electron*. 2009; 24(7): 1737–1746.
[2]  M Hagiwara, K Nishimura, H Akagi. A medium-voltage motor drive with a modular multilevel PWM inverter. *IEEE Trans. Power Electron*. 2010; 25(7): 1786–1799.
[3]  H Akagi. Classification, Terminology, and Application of the Modular Multilevel Cascade Converter (MMCC). *IEEE Trans. Power Electron*. 2011; 26(11): 3119–3130.
[4]  H Peng, M Hagiwara, H Akagi. Modeling and Analysis of Switching-Ripple Voltage on the DC Link Between a Diode Rectifier and a Modular Multilevel Cascade Inverter (MMCI). *IEEE Trans. Power Electron.* 2013; 28(1): 75–84.
[5]  C Gao, X Jiang, Y Li, Z Chen, J Liu. A dc-link voltage self-balance method for a diode-clamped modular multilevel converter with minimum number of voltage sensors. *IEEE Transactions on Power Electronics.* 2013; 28(5): 2125-2139.
[6]  J Gholinezhad. Analysis of cascaded Analysis of Cascaded H-Bridge Multilevel Inverter in DTC-SVM Induction Motor Drive for FCEV. *Journal of Electrical Engineering and Technology*. 2013; 8(2): 304-315.
[7]  MR Banaei. Asymmetric Cascaded Multi-level Inverter: A Solution to Obtain High Number of Voltage Levels. *Journal of Electrical Engineering and Technology*. 2013; 8(2): 316-325.
[8]  MR Banaei. Reduction of Components in Cascaded Transformer Multilevel Inverter Using Two DC Sources. *Journal of Electrical Engineering and Technology*. 2012; 7(4): 538-545.